

Constraining AGN Feedback in Massive Ellipticals with South Pole Telescope Measurements of the Thermal Sunyaev-Zel'dovich Effect

Alexander Spacek, Evan Scannapieco, Seth Cohen, Bhavin Joshi, Philip Mauskopf

Arizona State University – aspacek@asu.edu

ASU SCHOOL OF EARTH & SPACE EXPLORATION
ARIZONA STATE UNIVERSITY

INTRODUCTION

Since $z \approx 2$, star formation has occurred in progressively less massive galaxies [4] and active galactic nuclei (AGN) have occurred around progressively less massive black holes [3], contrary to expectations from the hierarchical model of structure formation. The most successful models for this anti-hierarchical evolution invoke additional energy input, most likely feedback from AGN [7], but the total energy released by these processes remains largely unknown.

A promising approach to measuring AGN feedback is co-adding the cosmic microwave background (CMB) around a large number of sources to measure the signal imprinted by the thermal Sunyaev-Zel'dovich (tSZ) effect. Several recent studies have used this approach, making detections of galaxies at low redshifts ($z \approx 0.5$) and AGN from $z = 0-3$ [5,8,9,14]. These have motivated us to investigate the little-measured regime of relic AGN feedback in quiescent elliptical galaxies at moderate redshifts ($z = 0.5-1.5$).

METHODS AND DATA

The tSZ effect describes the process by which CMB photons gain energy when passing through ionized gas [16]. The resulting CMB anisotropy has a deficit of photons below 217.6 GHz and an excess of photons above. The change in CMB temperature at 150 GHz (our frequency of interest; ΔT_{150}) can be integrated around a source on the sky, and it becomes a volume integral of the electron pressure which is equivalent to a thermal energy (see Eq. 1).

$$E_{\text{therm}} = -1.102 \times 10^{60} \text{ ergs} \left(\frac{l_{\text{ang}}}{\text{Gpc}} \right)^2 \int \frac{\Delta T_{150}(\theta) d\theta}{\mu\text{K arcmin}^2} \quad \text{Eq. 1}$$

We made our tSZ measurements using data from the South Pole Telescope SZ Survey (SPT-SZ; [15]), which has sensitivities of 17 and 41 $\mu\text{K arcmin}$ at 150 GHz and 220 GHz, respectively, and a ≈ 1 arcmin beam that is well matched to the expected sizes of the heated regions. We created our own photometric catalog of galaxies using two surveys that overlap with the SPT-SZ data, including optical and infrared data from the Blanco Cosmology Survey (BCS; [6]) and infrared data from the VISTA Hemisphere Survey (VHS; [11]). The total overlap between the 3 surveys is $\approx 43 \text{ deg}^2$.

GALAXY SELECTION AND STACKING

We used $g-z$ vs. $z-K_s$ colors to cleanly separate ≥ 1 Gyr old galaxies at $0.5 \leq z \leq 1.5$ from stars and star-forming systems [1]. We used the routines EAZY [2] and FAST [10] to obtain best-fit model parameters for our galaxies. We made several cuts on these parameters to insure that we had selected massive, old, and quiescent galaxies, and we removed any galaxies that were likely to have contaminated tSZ measurements due to AGN, dust, and other factors. We further split the resulting galaxies into two redshift ranges, $0.5 \leq z \leq 1.0$ (“low- z ”) and $1.0 < z \leq 1.5$ (“high- z ”). We end up with 3394 galaxies at low- z and 924 galaxies at high- z . The parameters of the final galaxy sample are shown in Table 2.

z	$\langle z \rangle$	$\langle l_{\text{ang}}^2 \rangle$ Gpc ²	$\langle M \rangle$ M_{\odot}	$\langle \text{Age} \rangle$ Gyr	$\langle L_{Ks} \rangle$ erg s ⁻¹ Hz ⁻¹	$\langle z \rangle_M$	$\langle l_{\text{ang}}^2 \rangle_M$ Gpc ²
0.5 – 1.0	0.72	2.30	1.51×10^{11}	4.34	2.78×10^{30}	0.72	2.30
1.0 – 1.5	1.17	3.02	1.78×10^{11}	2.64	4.07×10^{30}	1.19	3.03

Table 2: Mean and mass-averaged parameters for final galaxy selection.

To make our stacked tSZ measurements, we optimally filtered the SPT-SZ maps and then summed and averaged the total signal within 0.5, 1, 1.5, and 2 arcmin radius apertures around our galaxies. Images of our final stacks are shown in Fig. 2. In order to understand the uncertainty in our measurements, we also performed an identical selection and stacking procedure around a large number of random points in our field. The final stacked signal measurements are given in Table 3.

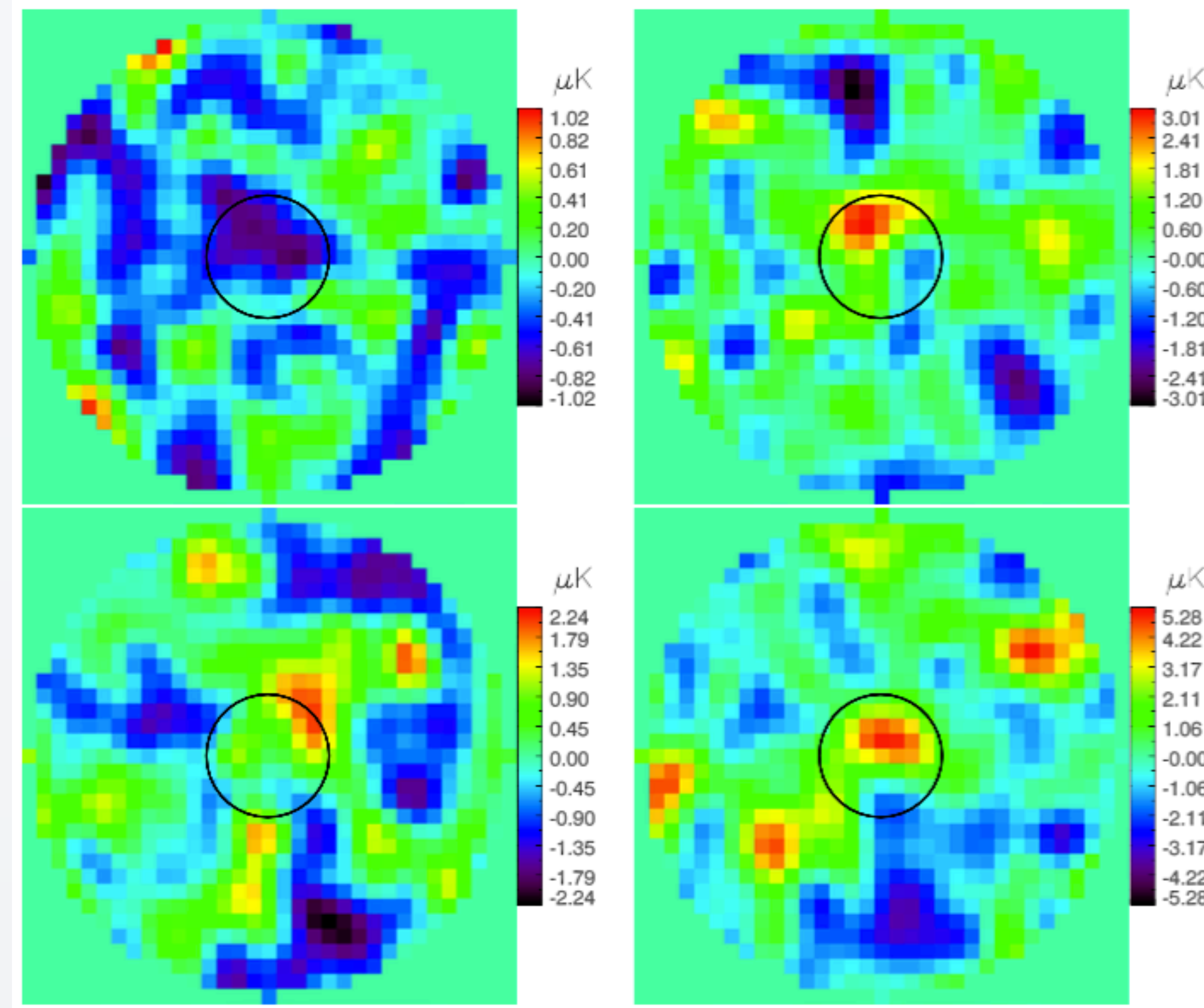


Fig. 2: Final stacked images. Left = 150 GHz, right = 220 GHz, top = low- z , bottom = high- z , black circles = 1 arcmin radius.

z	Band GHz	0.5 arcmin $\mu\text{K arcmin}^2$	1 arcmin $\mu\text{K arcmin}^2$	1.5 arcmin $\mu\text{K arcmin}^2$	2 arcmin $\mu\text{K arcmin}^2$
0.5 - 1.0	150	-0.56 ± 0.25	-1.6 ± 0.7	-2.5 ± 1.3	-3.0 ± 1.9
0.5 - 1.0	220	0.81 ± 0.54	2.9 ± 1.4	5.1 ± 2.3	5.9 ± 3.0
1.0 - 1.5	150	0.37 ± 0.49	1.6 ± 1.3	2.6 ± 2.4	2.8 ± 3.5
1.0 - 1.5	220	2.6 ± 1.0	6.2 ± 2.7	7.6 ± 4.3	6.9 ± 5.4

Table 3: Final co-add values for different aperture radii.

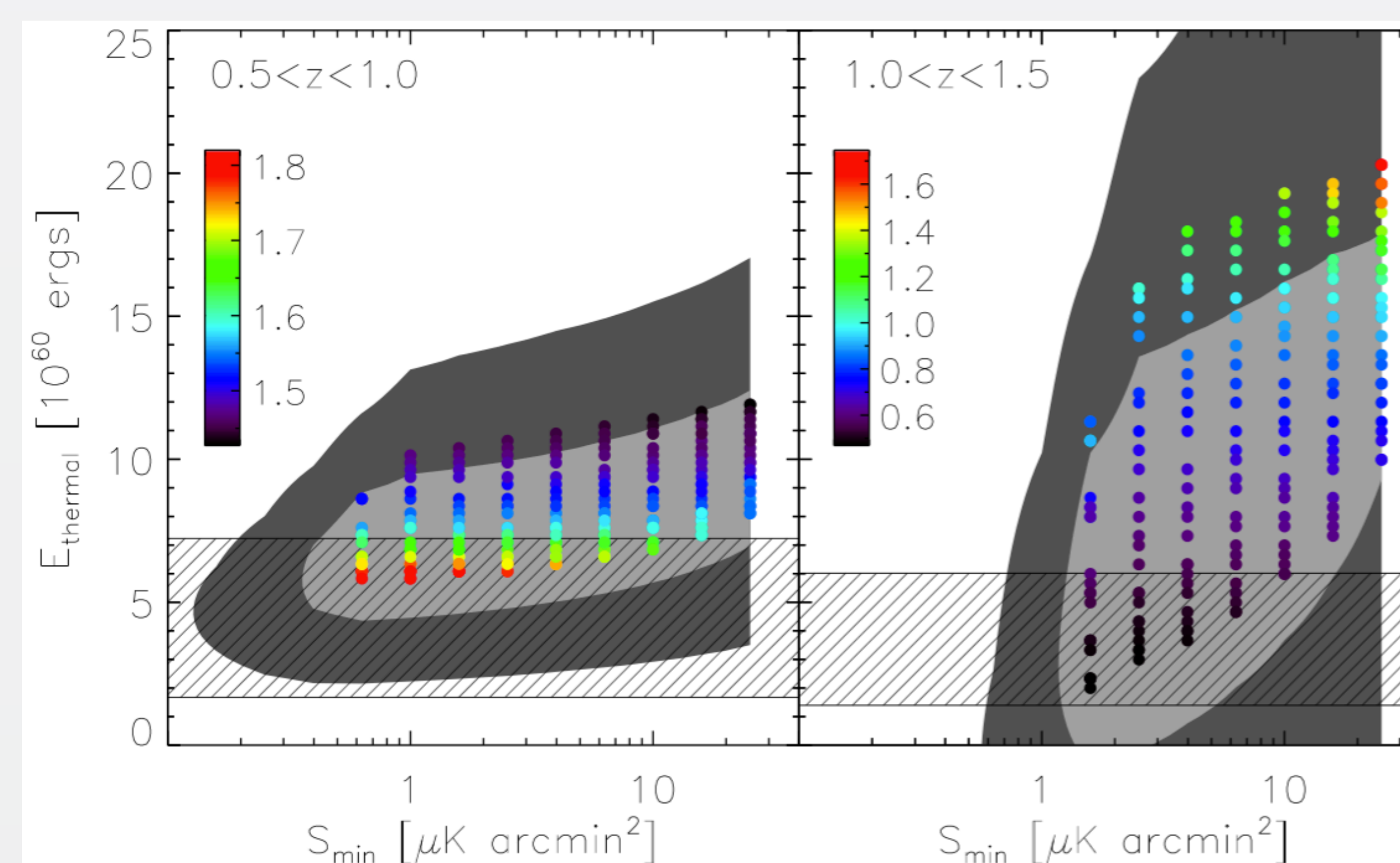


Fig. 3: Contaminant model confidence values for E_{thermal} as a function of S_{min} after incorporating Planck high-frequency bands. Light gray = 1σ range, dark gray = 2σ range. Colors represent the minimum χ^2 for each model. Hatched region represents $\pm 1\sigma$ for a simple model of gravitational heating.

CONTAMINATION MODELING

As can be seen in Fig. 2 and Table 3, there is a negative low- z signal at 150 GHz, as expected from the tSZ effect. At high- z the 150 GHz signal is roughly 0, but in both redshift ranges there is a very large positive signal at 220 GHz, indicating the presence of contaminating sources. In order to constrain the impact these sources have on our tSZ measurements we built a detailed model of contaminants based on an extrapolation of SPT source counts [12], and also made use of the 2015 public data release from the Planck mission [13], focusing on the 4 highest-frequency bands.

We obtained our final best-fit E_{thermal} values, shown in Fig. 3, by minimizing χ^2 for the measured and model signals while varying the minimum allowed contaminant flux (S_{min}), tSZ signal, fraction of our galaxies that are contaminated, contaminating dust temperature, and residual primary CMB anisotropy. The confidence of each model is then weighted by the minimum χ^2 for that model. The best-fit tSZ and E_{thermal} values after averaging across all varied parameters while incorporating the Planck data are shown as “With Planck” in Table 4.

Model	N	z	$\int \Delta T_{150}(\theta) d\theta$ $\mu\text{K arcmin}^2$	Y 10^{-7} Mpc^2	$E_{\text{therm}}(\pm 1\sigma)$ 10^{60} ergs	$E_{\text{therm}}(\pm 2\sigma)$ 10^{60} ergs
Data only	3394	0.5 – 1.0	-1.6 ± 0.7	1.2 ± 0.5	4.0 ± 1.8	4.0 ± 3.6
	924	1.0 – 1.5	1.6 ± 1.3	-1.2 ± 1.0	-5.3 ± 4.3	-5.3 ± 8.6
χ^2 (SPT only)	3394	0.5 – 1.0	$-3.1^{+1.1}_{-1.4}$	$2.3^{+1.0}_{-0.8}$	$7.9^{+3.5}_{-2.8}$	$7.9^{+7.8}_{-5.6}$
	924	1.0 – 1.5	$-2.0^{+1.5}_{-2.7}$	$2.0^{+2.6}_{-2.6}$	$6.7^{+8.9}_{-8.4}$	$6.7^{+20.3}_{-15.7}$
χ^2 (With Planck)	937	0.5 – 1.0	$-2.8^{+1.0}_{-1.2}$	$2.1^{+0.9}_{-0.7}$	$7.1^{+3.0}_{-2.5}$	$7.1^{+7.6}_{-4.8}$
	240	1.0 – 1.5	$-2.1^{+2.1}_{-2.7}$	$2.1^{+2.7}_{-2.1}$	$7.0^{+9.0}_{-7.0}$	$7.0^{+20.3}_{-13.3}$

Table 4: Final 1 arcmin radius aperture values for various modeling choices. “Data only” represents our raw co-adds, “SPT only” represents the best-fit values without incorporating Planck data, and “With Planck” represents the same values after incorporating Planck data.

DISCUSSION

Around our selection of galaxies, we find a stacked tSZ detection in our low- z subset ($0.5 < z < 1.0$) of $> 2\sigma$ significance. Our best-fit values after modeling the observed dusty contamination while incorporating Planck data improve to close to 3σ significance at low- z and 1σ at high- z ($1.0 < z < 1.5$). These correspond to thermal energies of $7.1^{+3.0}_{-2.5} \times 10^{60}$ ergs at low- z and $7.0^{+9.0}_{-7.0} \times 10^{60}$ ergs at high- z . We see a similar or smaller tSZ signal than most previous work on both AGN and galaxies [5,9,14], though not all [8]. Based on a simple model of gravitational heating, our low- z measurement hints at non-gravitational heating at the $\approx 1\sigma$ level.

Finally, tSZ simulations and observations can be combined to produce weighted stacks that are adapted to be as sensitive as possible to the differences between feedback models, which will be an important use for the results presented here. We are only just beginning to map out the history of AGN feedback through measurements of the thermal Sunyaev-Zel'dovich effect.

REFERENCES

- [1] Arcila-Osejo, L., & Sawicki, M. 2013, MNRAS, 435, 845
- [2] Brammer, G. B., van Dokkum, P. G., & Coppi, P. 2008, ApJ, 686, 1503
- [3] Buchner, J., Georgakakis, A., Nandra, K., et al. 2015, ApJ, 802, 89
- [4] Bundy, K., Ellis, R. S., & Conselice, C. J. 2005, ApJ, 625, 621
- [5] Chatterjee, S., Ho, S., Newman, J. A., & Kosowsky, A. 2009, ArXiv e-prints, arXiv:0908.3206
- [6] Desai, S., Armstrong, R., Mohr, J. J., et al. 2012, ApJ, 757, 83
- [7] Feldmann, R., & Mayer, L. 2015, MNRAS, 446, 1939
- [8] Gralla, M. B., Crichton, D., Marriaga, T. A., et al. 2014, MNRAS, 445, 460
- [9] Greco, J. P., Hill, J. C., Spergel, D. N., & Battaglia, N. 2014, ArXiv e-prints, arXiv:1409.6747
- [10] Kriek, M., van Dokkum, P. G., Labbe, I., et al. 2009, ApJ, 700, 221
- [11] McMahon, R. 2012, in Science from the Next Generation Imaging and Spectroscopic Surveys, 37
- [12] Mocanu, L. M., Crawford, T. M., Vieira, J. D., et al. 2013, ApJ, 779, 61
- [13] Planck Collaboration, Adam, R., Ade, P. A. R., et al. 2015, ArXiv e-prints, arXiv:1502.01582
- [14] Ruan, J. J., McQuinn, M., & Anderson, S. F. 2015, ApJ, 802, 135
- [15] Schaffer, K. K., Crawford, T. M., Aird, K. A., et al. 2011, ApJ, 743, 90
- [16] Sunyaev, R. A., & Zel'dovich, Y. B. 1970, Ap&SS, 7, 3